LA-UR-01-5168

*Approved for public release;
distribution is unlimited.*

c.1

Title: Measurements of the H(n,n)H Angular Distribution at 10 MeV Neutron Energy

Author(s): N. Boukharouba, F. B. Bateman, C. E. Brient,
A. D. Carlson, S. M. Grimes, R. C. Haight,
T. N. Massey and O. A. Wasson

Submitted to: International Conference on Nuclear Data for Science and Technology, Tsukuba, Ibaraki, Japan, October 7-12, 2001

Los Alamos
NATIONAL LABORATORY

Measurements of the H(n,n)H Angular Distribution at 10 MeV Neutron Energy

Nourredine BOUKHAROUBA[1,2], Fred B. BATEMAN[1,3,4], Charles E. BRIENT[1], Allan D. CARLSON[5,*],
Steven M. GRIMES[1], Robert C. HAIGHT[3], Thomas N. MASSEY[1] and Oren A. WASSON[5]
[1]*Institute of Nuclear and Particle Physics, Department of Physics and Astronomy, Ohio University, Athens, OH 45701*
[2]*Present address: Department of Physics, Chemistry & Physics Building, University of Kentucky, Lexington, KY 40506*
[3]*Los Alamos National Laboratory, Los Alamos, NM 87545*
[4]*Present address: National Institute of Standards and Technology, Gaithersburg, MD 20899*
[5]*National Institute of Standards and Technology, Gaithersburg, MD 20899*

Relative measurements of the cross section for scattering of neutrons by protons have been made at 10 MeV neutron energy for center-of-mass neutron scattering angles from 60° to 180°. The measurements were made using the Ohio University Accelerator Laboratory's tandem Van de Graaff accelerator with the D(d,n) reaction as the neutron source. The data are in good agreement with predictions from the phase shift analyses of Arndt, the groups of Nijmegen and Bonn, and the ENDF/B-V evaluation. The ENDF/B-VI evaluation does not appear to have the same angular dependence as the data.

KEYWORDS: hydrogen cross section, neutron cross section standard, hydrogen angular distribution standard, 10 MeV neutron energy, D(d,n) reaction, ENDF/B-V, ENDF/B-VI

I. Introduction

The H(n,n) interaction is one of the most fundamental processes in nuclear physics. Improving the accuracy of the np scattering cross section is important for a better understanding of the nucleon-nucleon interaction and for the resulting improvement in this important neutron cross section standard. This cross section is often referred to as the primary standard since so many neutron cross section standards are measured relative to it. Improvements in this cross section are needed in order to to refine theoretical calculations and phase shift analyses. The uncertainty in the results obtained from such work is affected by the limited database.

Despite the importance of the np scattering angular distribution as a standard, there is some disagreement concerning its behavior at neutron energies below 15 MeV. The available data sets are clustered around 14 MeV, and generally characterized by large error bars. Despite these large uncertainties, these data sets differ with each other significantly. Furthermore, the two most recent ENDF evaluations of the n-p elastic scattering data are strongly influenced by the data obtained at 14 MeV. They show disagreements of about 2% at 10 MeV for the important cross section at 180° in the center-of-mass system. This angle, which corresponds to proton recoils at 0° in the laboratory system, is the most important angle for use of this cross section as a standard or for neutron fluence determination.

To improve our knowledge of this important cross section, test the various predictions, and provide data for a new evaluation of this cross section, the present measurements were made of the shape of the hydrogen differential cross section at 10 MeV neutron energy with an accuracy of ~1%. These measurements were made at the Institute of Nuclear and Particle Physics at Ohio University. This work is a continuation of earlier measurements[1)] by this collaboration. The new measurements incorporate many changes in the experiment to provide results with smaller systematic errors. Significant improvements were made in the hydrogenous target, electronics, data acquisition systems, collimators and analysis process compared with those used in our previous work.

II. Experimental Details

1. The Scattering Chamber

A multi-telescope scattering chamber was designed especially for this experiment. A diagram of the experimental setup showing the scattering chamber is shown in **Fig. 1**.

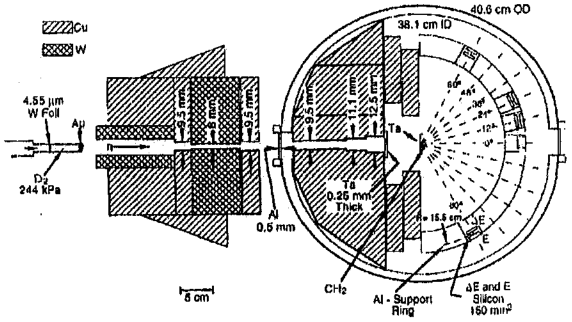

Fig. 1 Experimental setup for the np scattering measurement

Proton recoils from neutrons striking a hydrogenous target were detected in proton telescopes each composed of a pair of surface barrier solid state detectors, ΔE and E, operated in coincidence in order to lower the backgrounds. All detectors had an active area of 150 mm^2. Data were obtained

---

* Corresponding author, Tel. +1-301-975-5570, Fax. +1-301-975-4766, Email: carlson@nist.gov

simultaneously with 11 ΔE-E telescopes positioned at 0°, ±12°, ± 24°, ±36°, ±48° and ±60° relative to the neutron beam axis. This corresponds to the angular range from 180° to 60° degrees in the center-of-mass system for neutrons.

Nearly all previous measurements have utilized a single telescope which was used sequentially to obtain an angular distribution by rotating it to various angles relative to the direction of the incident neutron beam. These experiments require very accurate monitoring of the neutron beam intensity. Another difficulty with this procedure is that the thicknesses of the ΔE and E detectors cannot be optimized for all angles. For the present experiment, the detector thickness for both the ΔE and E counters were individually tailored to each angle.

Having telescopes on both sides of the neutron beam axis provides a good way to monitor any asymmetry in the neutron beam, hydrogenous target, or in the alignment. In addition to allowing more flexibility in the choice of detector thickness, the multi-telescope spectrometer increases the data acquisition rate. It averages out left-right asymmetries, and provides a redundant set of independent measurements which will decrease the overall uncertainty.

The scattering chamber, neutron collimation, and target were carefully aligned with the beam line, using an optical telescope and a laser beam. The scattering angles for each telescope were obtained with an estimated accuracy of ±0.1°.

The solid angle for each telescope was defined by a collimator held firmly against the front of the ΔE detector (the detector closer to the polypropylene target) by a tight-fitting aluminum sleeve. An additional larger collimator was placed between the ΔE and E detectors. This arrangement allowed the relative solid angles of the telescopes to be determined in a reliable way, without the necessity of opening the scattering chamber and removing the ΔE detectors. For all angles other than 60°, the front solid-angle defining circular collimator had an inner radius of 0.47 cm, while the second larger collimator had an inner radius of 0.6 cm. The 60°-collimator was in the shape of a rectangular aperture with rounded corners. The smaller dimension of the rectangle was positioned in the horizontal plane in order to reduce the angular acceptance of the telescope. This configuration substantially decreases the kinematic spread which is important at this angle, and yields sharper recoil proton peaks.

Relative solid-angle values for all telescopes were obtained by counting with a very thin and uniform (± 0.5% variation over a 12.7 mm diameter) ^{239}Pu alpha-particle source, placed at the sample position which had an area similar to that of the hydrogen scattering sample. This experiment did not require absolute solid-angle measurements since the shape of the angular distribution was being measured.

The hydrogenous targets were made with a circular film of commercial treated polypropylene (CH_2) 1 cm in diameter attached to a 0.5 mm thick tantalum plate, and facing the ΔE -E telescopes. The tantalum plate was used as a target support which helped keep the surface of the target flat. A flat surface was especially important for the larger angles where a wavy film would induce a distortion in the recoil proton yield. The targets were bonded to the tantalum backing with a thin layer of ethyl cyanoacrylate. The charged particles produced from neutron interactions with nuclides other than hydrogen in the target and ethyl cyanoacrylate have less than a 0.1% calculated effect on the cross sections obtained in the experiment.

Because of the large recoil-proton energy difference between the small and the large angles, two thicknesses were used in the experiment: a thick sample (3.8×10^{-3} g/cm^2) for all angles except 60° to enhance the signal/background ratio, and a thin sample (1.4×10^{-3} g/cm^2) for all angles. This thin sample was required for the 60° angle where a minimum energy-loss in the sample was desired. These films needed only to be analyzed for impurities, which were negligibly small, and not for absolute hydrogen content.

2. Neutron Source and Collimation

10 MeV neutrons for the experiment were obtained from the D(d,n) neutron source reaction using a 4.2 cm gas cell maintained at a pressure of 276 kPa (40 psi). The Ohio University tandem Van de Graaff accelerator provided the deuteron beam with currents of about 8 μA. A 4.1 μm thick tungsten foil separated the deuterium gas from the accelerator vacuum.

The neutron beam was collimated with blocks of copper and tungsten, as shown in Fig. 1, such that the neutron fluence over the CH_2 target was uniform and slightly larger in size than the target. A radiograph verified the position and uniformity of the neutron beam. Neutron transport calculations were used in the design of the neutron shielding and collimation system. The collimation close to the target was needed to sharpen the edges of the neutron beam radial profile, and to reduce the number of events in the silicon ΔE-E telescopes from neutron-induced charged-particle producing reactions in the detectors, which might be recorded as true recoil-proton events. A sheet of tantalum covered the collimator to stop the charged particles produced in the aluminum entrance window of the chamber and the neutron-collimation materials.

Deuteron-breakup in the gas cell was investigated in a separate experimental run using a ^{3}He-filled gas cell, and was found to be negligible.

3. Data Acquisition

Signals from the electronics were sent to two separate data acquisition systems, each using a separate personal computer. This reduced possible problems with the total counting rate associated with the 22 individual detectors if they had all been used with one acquisition system and computer. One system stored the data for the 0°, ± 12° and ± 24° detectors. It was called the "fast" system since the timing signals for that system were obtained from discriminators connected directly to the fast signal outputs of the preamplifiers which were used. This is appropriate for the higher energy proton recoil pulses produced at these angles. The other system stored data for all detectors except those at the 0° angle. It was called the "slow" system since the timing signals for that system were obtained from discriminators connected to the amplified and shaped output of the preamplifiers. This system is appropriate for the lower energy proton recoil pulses produced at these angles. The storing of data for the ± 12° and ± 24° telescopes in both computers allowed the two data acquisition systems to be normalized with no concerns about uncertainties in the calculation of dead time losses. Also this redundancy allowed consistency checks to be made.

For each system, timing and pulse-height signals from the various detectors were multiplexed into a separate ADC-computer system. Pulse-height, timing, router, and neutron monitor signals were stored in an event buffer, and subsequently written to disk for later off-line sorting and analysis. A coincidence between ΔE and E signals was performed in hardware in order to minimize the background due to stray random events. Further background reduction was obtained by using the timing signals from each set of ΔE and E detectors to generate relative timing information.

A time-of flight (TOF) signal was used to gate the event stream during off-line analysis. The purpose of this gate was to eliminate those events which meet the ΔE-E coincidence requirement, but fall outside the time window defined by the TOF gate. It was most helpful for the 0° and 12° scattering angles, where background levels are high and the rate of random ΔE-E coincidence occurrences was higher.

II. Data Analysis and corrections

The digitized events were sorted for each detector and protons were identified from the E-ΔE plots. Legitimate events were those corresponding to protons with the appropriate energy which satisfy a restriction imposed by setting a TOF gate on all events that met the particle-type and energy requirements.

The data sets consisted of several runs for both thin and thick target measurements, along with the corresponding background or blank runs. Event data from the "slow" and the "fast" systems were treated as independent measurements and analyzed separately, then normalized to each other in the final stages of the analysis to obtain the complete relative angular distribution for a given target thickness. The normalization constant in this case was obtained from the average ratio of the proton yields for the telescopes at ± 12° and ± 24° for the "slow" and "fast" systems.

Recoil proton yields were obtained from raw two-dimensional E vs. ΔE and E vs. TOF scatter plots by drawing polygonal gates around the region of interest. This procedure was followed for both the foreground and the background data. Various E-ΔE and E-TOF gates of reasonable sizes and shapes were utilized to obtain the raw proton yields. Upon comparison, it appeared that these yields were, to a large extent, independent of any particular set of gates, except at 0° where a maximum of 0.9% difference in proton yield was obtained for different sets of E-ΔE gates. This was expected because of the larger level of background events for this telescope, which was directly in the path of the neutron beam. Because of straggling, the 48° and 60° ΔE detectors exhibited a residual tail in the recoil proton peak after background subtraction.

To alleviate this problem, the E and ΔE signals from the raw data were gain matched using a Monte Carlo (MC) program, described below, then summed to obtain the total recoil energy for each event. This resulted in a reduction of the residual tail to about 0.6% of the total peak sum for the 60° right telescope, and only 0.2% for the 60° left telescope.

Stilbene neutron monitor rates determined the normalization factor used in the subtraction of the background from the foreground data. Relative solid angle normalization was applied to the background-corrected recoil proton yields using the relative solid angle values obtained from the ^{239}Pu alpha source measurements.

The MC simulation program was written to assist in the design and analysis of this experiment, and to ascertain proton-loss mechanisms. With this program proton recoils were traced from their origin to point of detection, including scattering from carbon and hydrogen atoms within the target, and then, from the silicon atoms in the detectors. Statistics for the number of straight-line proton trajectories were stored, as well as those including atomic collisions. The percentage of proton losses due to multiple scattering, and the finite-geometry effects were estimated from the comparison of these two statistics.

This program calculated many of the relevant parameters such as energy loss of the recoiling proton in the CH_2 sample and ΔE detectors, solid angles subtended by the detectors at the target, effective scattering angles due to the finite target size, and straggling. Various tests were made of the MC program which indicated it was working properly.

Calculations of proton counting losses from nuclear reactions in silicon at the proton energies under consideration showed that these were less than 0.1%.

All corrections were then carried out individually for each detector and each target thickness. The results showed good agreement between the beam-right and beam-left values.

Relative angular distributions were obtained for each target thickness after averaging the beam-left and beam-right values. These distributions were then transformed to the center-of-mass system using relativistic kinematics. The thin and thick target data were then combined, fitted with a Legendre polynomial, integrated, and finally normalized to the total elastic cross section given in ENDF/B-V.

III. Results

The present angular distribution data are shown in **Fig. 2** compared with the ENDF/B-V[2)] and ENDF/B-VI[3)] data evaluations, results from the CD-Bonn[4)] and Nijmegen[5)] potentials, and the Arndt-SM94 phase-shift analysis[6)].

Estimated uncertainties for the present measurements in the center-of-mass angular range from 180° to 60° are 0.6%

to 1.4% for the foreground uncertainty, 0.2% to 0.8% for the background uncertainty, 0.5% to 0.1% for the gate size uncertainty and 0.8% to 1.7% for the total uncertainty. Other sources of uncertainty such as MC corrections, foreground-background normalization and solid angle uncertainties are included in the total uncertainty.

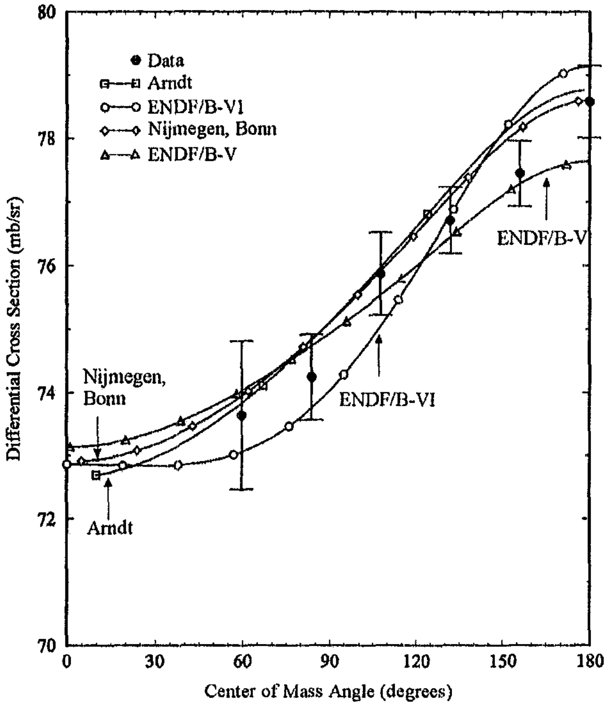

Fig. 2 Present measurements of the H(n,n) angular distribution at 10 MeV neutron energy compared with Arndt-SM94, Nijmegen, CD-Bonn, ENDF/B-V and ENDF/B-VI results

Good agreement with the present data was found with the results from the CD-Bonn and Nijmegen potentials, the Arndt-SM94 phase-shift analysis and the ENDF/B-V data evaluation. There was somewhat better agreement for the CD-Bonn model and Arndt partial-wave analysis results. The ENDF/B-VI angular distribution does not appear to have the right angular dependence at this energy. Furthermore, its total cross section predictions are lower than most of the experimental data at this energy.

The ENDF/B-VI evaluation was strongly influenced by measurements$^{7)}$ at about 14 MeV neutron energy. The publication of this work has been investigated and some serious problems were found with the analysis of that experiment. Pulse height distributions for the foreground and background data indicate that there were tails, events of lower pulse height, which have not been explained. It was difficult to evaluate errors associated with this. Also, the measurements were made at a time when it was difficult to make corrections for the effects resulting from proton scattering in the polyethylene target and the proportional counters used in the experiment. Unfortunately, the publication does not contain all the information necessary to calculate these corrections. Assuming that the diagram of the counter telescope was drawn to scale, an estimate of the error introduced by not including these corrections was obtained with the MC program used in the present experiment. This error is tentatively estimated at 2%. This error should be added in quadrature with the uncertainties shown for each data point in the publication. This will represent a lower limit since we have not assigned an error from the tails in the pulse height distribution. Additionally, errors were found in the center-of-mass angles used in their analyses, which we have corrected. In summary, uncertainties in the results of Nakamura$^{7)}$ are larger than previously reported.

IV. Conclusion

We have measured the shape of the H(n,n) scattering angular distribution between 60° and 180° in the center-of-mass system with an average uncertainty of better than 0.8%. The present data support the validity of the potentials of the Bonn and Nijmegen groups, the phase-shift analysis of Arndt, and the ENDF/B-V evaluation. The poorer agreement with ENDF/B-VI suggests there may be problems with the accuracy of some data$^{7)}$ at 14 MeV.

Acknowledgments

The authors acknowledge the assistance of D.E. Carter for his help with the electronics and data acquisition, D. Sturbois for accelerator maintenance, and J.E. O'Donnell, R. Wheeler and J. Oldendick for help with accelerator operations. We would also like to thank Prof. C. Elster for her help in the phase-shift calculations, and Dr. D. Gilliam for supplying the ^{239}Pu alpha source. This work was supported in part by the U.S. Department of Energy.

References

1) R.C. Haight, F.B. Bateman, S.M. Grimes, C.E. Brient, T.N. Massey, O.A. Wasson, A.D. Carlson and H. Zhou, "Measurement of the Angular Distribution of Neutron-Proton Scattering at 10 MeV," *Fusion Engineering and Design* **37**, 49 (1997).
2) L. Stewart, R.J. LaBauve and P.G. Young, "Summary Documentation for H" in "ENDF/B-V Summary Documentation," ENDF-201, (BNL-NCS-17541), Brookhaven National Laboratory (1979).
3) G.M. Hale, D.C. Dodder, E.R. Siciliano and W.B. Wilson, "Summary Documentation for H" in "ENDF/B-VI Summary Documentation," ENDF-201 (BNL-NCS-17541), Brookhaven National Laboratory (1991).
4) R. Machleidt, "High-precision, charge-dependent, Bonn nucleon-nucleon potential," *Phys. Rev.* **C63**, 024001 (2001)
5) J.J. de Swart, R.A.M.M. Klomp, M.C.M. Rentmeester and Th.A. Rijken, "The Nijmegen Potentials," *Few-Body Systems Suppl.* No. 8, 438 (1995).
6) R.A. Arndt, I.I. Strakovsky and R.L. Workman, "Updated analysis of NN elastic scattering data to 1.6 GeV," *Phys. Rev.* **C50**, 2731 (1994).
7) T. Nakamura, "Angular Distribution of n-p Scattering at 14.1 MeV," *J. Phys. Soc. Japan* **15**, 1359 (1960).